Clinical Radiology 74 (2019) 815.e1–815.e7

Contents lists available at ScienceDirect

Clinical Radiology

journal homepage: www.clinicalradiologyonline.net

Detection of bone marrow oedema in knee joints using a dual-energy CT virtual non-calcium technique

M.-Y. Wang [1], X.-Y. Zhang [1], L. Xu [1], Y. Feng, Y.-C. Xu, L. Qi*, Y.-F. Zou*

Department of Radiology, The First Affiliated Hospital of Nanjing Medical University, Nanjing, People's Republic of China

ARTICLE INFORMATION

Article history:
Received 16 March 2019
Accepted 26 June 2019

AIM: To evaluate bone marrow oedema in knee joints quantitatively and qualitatively using a dual-energy computed tomography (CT) virtual non-calcium (VNCa) technique.

MATERIALS AND METHODS: Thirty-five patients with knee joint injuries underwent both dual-energy CT and magnetic resonance imaging (MRI) between March 2018 and November 2018. The presence of bone marrow oedema was assessed by two independent radiologists with the use of colour-coded dual-energy CT VNCa images and measured attenuation on them. The biggest area of bone marrow oedema on axial images was measured by another radiologist using the dual-energy CT and MRI images, respectively. Attenuation values were subjected to receiver operating characteristic (ROC) curve analysis and oedema area sizes were subjected to paired *t*-test analysis.

RESULTS: In qualitative analysis, colour-coded VNCa images had an overall sensitivity of 88.4%, specificity of 98%, positive predictive value of 92.7%, negative predictive value of 96.8%, and accuracy of 95.9%. Attenuation values obtained from colour-coded VNCa images were significantly different in knee joint regions with and without oedema ($p<0.001$). ROC curve analysis revealed an area under the curve (AUC) of 0.910. A cut-off value of −67 HU provided a sensitivity of 81.4%, specificity of 99.3%, accuracy of 90.4%, positive predictive value of 99.1%, and negative predictive value of 84.2% for the differentiation of oedematous knee joint regions. Significant differences in the size of oedema area were not found between them.

CONCLUSION: Dual-energy CT VNCa can be used to evaluate bone marrow oedema effectively.

Introduction

The knee joint is the largest and most complex joint in the human body, consisting of the femur, tibia, and patella, with many tendons and ligaments around it. It plays a major load-bearing role in the human body, which is easily injured. Bone marrow oedema in the knee joint shows increases of interstitial fluid and blood. It is associated with

* Guarantor and correspondent: L. Qi and Y.-F. Zou, Department of Radiology, The First Affiliated Hospital of Nanjing Medical University, 300 Guangzhou Road, Gulou District, Nanjing, People's Republic of China. Tel./fax: +86-25-83724440, +86-25-83673427.

E-mail addresses: qiliang1120@126.com (L. Qi), zouyuefendc@126.com (Y.-F. Zou).

[1] These authors contributed equally to this work.

https://doi.org/10.1016/j.crad.2019.06.020
0009-9260/

many disease states including trauma, infections, degenerative arthritis, neoplasia, and "transient osteoporosis".[1,2] The early diagnosis of bone marrow oedema in knee joints can provide reasonable clinical explanations for joint pain, and suggests that patients should reduce their activities to prevent complications.

Bone marrow oedema is frequently identified at magnetic resonance imaging (MRI) described as geographic or reticulated areas of low signal intensity on T1-weighted MRI images and high signal intensity on T2-weighted MRI images in the bone marrow. Unfortunately, there are some contraindications to MRI, such as pacemaker devices or claustrophobia, and the duration of examination is long and might be unbearable for some trauma patients.[3–5] Compared with MRI, CT has the advantages of shorter scanning time and depiction of subtle cortical fracture; however, the dense trabecular structure of the cancellous bone impedes the visualisation of bone marrow oedema at conventional single-energy CT.[6,7] Continuous development of dual-energy CT makes visual evaluation of bone marrow oedema feasible with virtual non-calcium (VNCa) images.[6,8–10] Previous investigators have used this method in the extremities and spine, and successfully detected bone marrow oedema with first-generation or second-generation dual-energy CT systems.[11–16] Third-generation dual-energy CT has a higher spectral resolution compared to the previous generations, and therefore, may provide more information for bone marrow. The VNCa technique using the latest generation of dual-energy CT could be used to evaluate bone marrow qualitatively and quantitatively in the knee joints. Thus, the aim of the present study was to assess the feasibility and accuracy of the VNCa technique at third-generation dual-energy CT for detection of bone marrow oedema in traumatic knee joints.

Materials and methods

Study population

The present prospective study was approved by the clinical research ethics board and informed consent was obtained from all patients. Between March 2018 and November 2018, 46 consecutive patients with knee joint injuries who underwent CT as a result of inconclusive radiography or to evaluate fracture extent to determine treatment were enrolled in this study. The exclusion criteria were as follows: pregnancy, any contraindications to MRI, and metal implants or diseases affecting bone marrow attenuation. Seven patients were excluded because of claustrophobia (n=1), implant pacemaker (n=2), and severe artefacts of metal implants on the MRI images (n=2), and neoplastic disease (n=2). Finally, thirty-nine patients (36.3±16.9 years; age range, 13–89 years) were included in this study. There were 22 men (40.4±15.8 years; age range, 21–89 years) and 17 women (30.7±17.3 years; age range, 13–65 years). MRI was performed as soon as possible after dual-energy CT.

Dual-energy CT protocol

All CT examinations were conducted using a third-generation dual-energy CT system (Somatom Force; Siemens Healthcare, Erlangen, Germany) equipped with two X-ray tubes (tubes A and B with two different voltages). Acquisitions of the injured knee joint images were performed with a dual-energy protocol in a craniocaudal scan direction. The dual-energy CT examination parameters used were as follows: tube A: tube voltage of 80 kV, reference current–time product of 250 mAs; tube B: Sn150 kV, where Sn indicates the use of an integrated tin filter; reference current–time product of 150 mAs, 128×0.6 mm collimation, 0.6 pitch, 0.5 seconds rotation time. Real-time automatic tube current modulation (CARE dose 4D; Siemens) was applied. The mean volume CT dose index of this protocol was 10.4±4.1 mGy (range, 3.8–16.9 mGy), and the mean dose–length product was 321.4 mGy·cm (range, 87.3–921.8 mGy·cm). These dose parameters are comparable to the standard CT protocol for the knee joint. Intravenous contrast material was not used in each patient.

CT image post-processing

After each knee joint CT examination, three different image sets were generated with a dual-energy system, 80 kVp, Sn 150 kVp with a tin filter, and a weighted average, which was calculated from both tube data at a ratio of 0.5:0.5 to reproduce the characteristics of a single-energy 120 kVp image set. Sagittal and coronal multiplanar reformations were created from the weighted average imaging with 2-mm-thick sections and 1-mm increments by using different kernels (B70f and D30f). Commercially available software (Syngo Dual Energy, version VB10B; Siemens Healthcare, Germany) was used for post-processing of images. VNCa images were generated from the software "bone marrow" application, which was based on a three-material decomposition algorithm for red marrow, yellow marrow, and bone mineral.[17,18] VNCa images were present in the form of colour-coded images (bone marrow setting in Syngo Dual Energy). Axial, sagittal, and coronal multiplanar colour-coded reformations were all created with a section thickness of 3 mm (increment, 0.7 mm) for further assessment and analysis.

MRI protocol

MRI examinations were conducted using a 3 T MRI unit (Magnetom Skyra Trio; Siemens Healthcare) with a knee joint coil. The MRI protocols included the following sequences: axial fat-saturated proton density weighted (3,500 ms repetition time [TR]/54 ms echo time [TE], 180×180 mm^2 field of view, 256×320 matrix, 4 mm section thickness, 0.8 mm gap), coronal spin-echo T1- weighted (430 ms TR/11 ms TE; 160×160 mm^2 field of view, 192×320 matrix, 3 mm section thickness, 0.6 mm gap), coronal fat-saturated fast spin-echo T2-weighted (3,500 ms TR/54 ms TE; 160×160 mm^2 field of view, 192×320 matrix, 3 mm section thickness, 0.6 mm gap), sagittal fat-saturated fast spin-echo

T2-weighted (3,500 ms TR/54 ms TE; 160×160 mm^2 field of view, 192×320 matrix, 3 mm section thickness, 0.6 mm gap), and sagittal fat-saturated proton density weighted (2,500 ms TR/21 ms TE; 160×145 mm^2 field of view, 192×320 matrix, 3 mm section thickness, 0.6 mm gap).

Image analysis

Three radiologists with >5 years of experience in musculoskeletal radiology participated in the image analysis. For subjective and objective image analysis, each knee joint was divided into five regions (lateral or medial femur, lateral or medial tibia and patella). There were a total of 195 assessable regions for the dual-energy colour-coded images and MRI images, respectively. Two radiologists reviewed each dual-energy colour-coded region independently in random order and were both blinded to patient clinical details and MRI findings. They evaluated whether oedema existed in the bone marrow or not. If oedema existed in the bone marrow, it displayed in green or yellow on the dual-energy colour-coded images, which was recorded as "1", otherwise it was recorded as "0". Oedema regions should have a distance of >2 mm from adjacent cortical bone to avoid interference from sclerotic bone changes and joint effusion.[11] If there is a disagreement among observers, consensus assessment was obtained and consensual results were used for further analysis. Then two readers chose circular regions of interest (ROIs) over each region independently on the dual-energy colour-coded images. The ROIs were placed at the location of highest oedema intensity, which was green or yellow on the colour-coded images, to obtain attenuation values. In other knee joint regions without oedema, an ROI was chosen randomly in the middle of the region. The sizes of ROIs were all >0.7 cm^2 and <0.8 cm^2.

The third reader evaluated the presence of bone marrow oedema on the MRI image regions. The reader was blinded to the dual-energy CT results. The reader identified three continuous sections with the biggest area of bone marrow oedema on axial fat-saturated fast spin-echo T2-weighted images, and drew the boundary round the area of oedema. The average area of the three sections was calculated and recorded. After a 4-week interval, the area of bone marrow oedema on the corresponding colour-coded CT images regions was measured by the same reader.

Statistical analysis

All the analyses were performed using statistical software (SPSS Statistics for Windows, version 20.0; IBM, Armonk, NY, USA). Continuous variables were analysed using the *t*-test. A *p*-value of <0.05 was considered to indicate a statistically significant difference. Interobserver agreements for qualitative analysis were calculated by using weighted κ statistics.[19,20] Consensus data from qualitative assessment of dual-energy colour-coded images and data from MRI were used to calculate the sensitivity, specificity, accuracy, positive predictive value, and negative predictive value.

The ROC curve analysis and calculations of the AUC were used to assess the attenuation values from dual-energy CT VNCa images, taking MRI as the reference standard. High attenuation values were considered signs of bone marrow oedema. Interobserver agreement for ROI-based attenuation was assessed with the interclass correlation coefficient (ICC). Then, averaged ROI-based attenuation values were compared with MRI images by means of ROC analysis. The cut-off attenuation value derived from the ROC analysis showed the highest accuracy for the presence or absence of bone marrow oedema. Then sensitivity, specificity, accuracy, positive predictive value, and negative predictive value were calculated.

The average area obtained from the three sections from the dual-energy CT and MRI images are analysed using pair *t*-tests.

Results

Dual-energy CT and MRI were performed within a mean of 2.1 days (range, 0–5 days) of each other. MRI revealed a total of 43 oedematous knee joint regions (43/195, 22%) and 152 non-oedematous knee joint regions (152/195, 78 %).

The overall interobserver agreement for qualitative analysis of dual-energy colour-coded images was excellent (κ=0.882). A consensus of oedema evaluation on dual-energy CT colour-coded images was required in seven knee joint regions. Taking MRI as the reference standard, three false-positive bone marrow oedema regions were found on dual-energy CT colour-coded images, on the other side, five false-negative bone marrow oedema regions were found (Table 1). A total sensitivity of 88.4%, specificity of 98%, positive predictive value of 92.7%, negative predictive value of 96.8%, and accuracy of 95.9% were obtained for oedema qualitative assessment on dual-energy CT colour-coded images (Figs 1 and 2).

An ICC for the interobserver agreement of ROI-based attenuation was 0.891, which indicated excellent agreement. Between oedematous and non-oedematous knee joint regions for each of the two readers, CT values on colour-coded images were significantly different ($p<0.001$; Table 2). The average CT values of oedematous knee joint regions were significantly increased for both reader 1 and reader 2 (Fig 3).

When ROC analysis was performed with dual-energy CT, the AUC was 0.911±0.033 for reader 1 and 0.910±0.034 for reader 2. When ROC analysis was performed with average dual-energy CT of the data from both readers, the AUC was 0.910±0.033 (Fig 4). Using a cut-off value of −67 HU

Table 1
Contingency table of qualitative assessment in knee joints with dual-energy computed tomography (CT) and magnetic resonance imaging (MRI)

Oedema status at MRI Imaging	Oedema status at CT	
	Oedema	No oedema
Oedema	38	5
No oedema	3	149

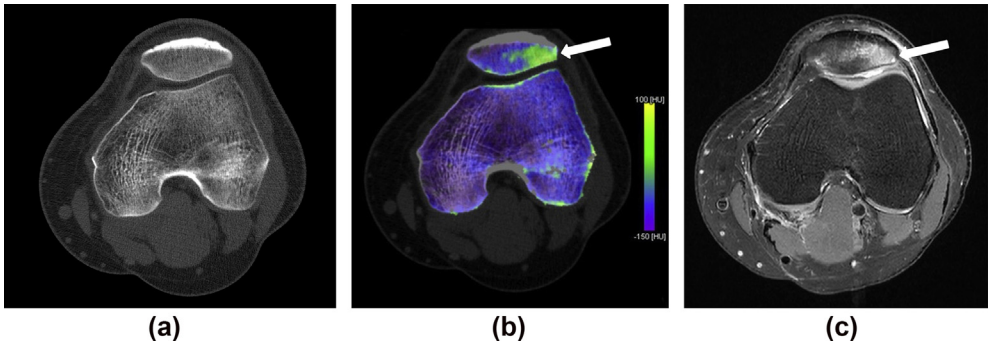

Figure 1 Images of a 39-year-old man after left knee joint trauma. (a) Axial weighted average dual-energy bone window CT image does not show obvious bone abnormality. (b) Corresponding colour-coded dual-energy VNCa image reveals bone bruising in the left patellar (white arrow). (c) Axial fat-saturated T2-weighted MRI image confirms bone contusion in the left patellar (white arrow), which is coded green in (b).

provided a total sensitivity of 81.4%, specificity of 99.3%, accuracy of 90.4%, positive predictive value of 99.1%, and negative predictive value of 84.2%.

MRI images show a total of 43 oedematous regions, but only 38 of them could be identified on the colour-coded dual-energy VNCa images. The areas of these 38 oedematous regions on the MRI and dual-energy CT images were analysed. Significant differences in the area of bone marrow oedema were not found between dual-energy CT and MRI images (p=0.061; Table 3).

Discussion

The prospective study evaluated bone marrow oedema in knee joints injuries using third-generation dual-energy CT, with MRI serving as the reference standard. The findings demonstrated dual-energy CT is able to assess bone marrow oedema in knee joints injuries virtually and quantitatively with subtracting calcium from the cancellous bone. This resulted in high specificity, high accuracy, high positive predictive value, and an excellent area under the ROC curve.

Dual-energy CT can differentiate various scanned materials based on the energy dependence of the photoelectric effect at different X-ray spectra and its dependence on the atomic number of substances.[8,18,21] By using a three-material decomposition model, VNCa images can be calculated with removal of calcium from CT data. A few studies have reported the use of the dual-energy VNCa images to assess bone marrow in the extremities and spine.[11–15] Guggenberger *et al.*[12] evaluated traumatic bone marrow oedema in the ankle with the use of 80 kV and Sn140 kV. Kellock *et al.* detected bone marrow oedema in non-displaced hip fractures with the use of 100 kVp and 140 kVp. Suh *et al.*[15] conducted a systematic review and meta-analysis with an electronic search of the PubMed and EMBASE databases. Their findings indicated that dual-energy CT has excellent sensitivity and specificity for bone marrow oedema detection.

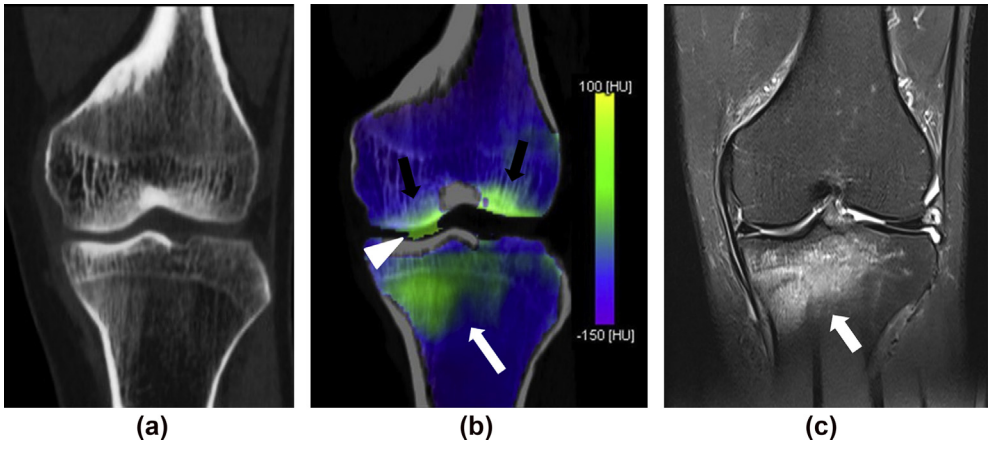

Figure 2 Images in a 49-year-old man with left knee joint post-traumatic pain and dyskinesia for 20 days. (a) Coronal weighted average dual-energy bone window CT image of the left knee joint does not show obvious bone abnormality. (b) Corresponding colour-coded dual-energy VNCa image reveals bone bruising in the left medial tibial plateau (white arrow). The green area (white arrowhead) in the joint space may be the artefact of joint effusion; another green area (black arrow) in the subarticular cortex of femoral condyle may be the artefact of osteosclerosis. (c) Coronal fat-saturated T2-weighted MRI image confirms bone contusion in the same region (white arrow), which is coded green in (b).

Table 2
Attenuation of the different knee joint regions on dual-energy virtual non-calcium images

Oedema status at MRI	Mean attenuation (HU)	
	Reader 1	Reader 2
Oedema (n=43)	−39.2±39.1	−38.4±40.7
No oedema (n=152)	−101.3±17.7	−104.2±16.6
p-Value[a]	<0.001	<0.001

[a]p-Values were calculated with the two-sample t-test; $p<0.05$ indicates a significant difference.

The latest generation dual-energy CT could decompose materials more precisely by using the new X-ray tube and made VNCa images more reliable. Wang *et al.*[13] used third-generation dual-energy CT with a 100 kV and Sn140 kV configuration for assessment of bone marrow oedema in the spine. Petritsch *et al.*[14]detected bone marrow oedema in vertebral compression fractures by using third-generation dual-energy CT with a 90 kV and Sn150 kV configuration. Their results are more promising than those reported with the use of dual-energy protocols in first or second-generation dual-source CT machines.

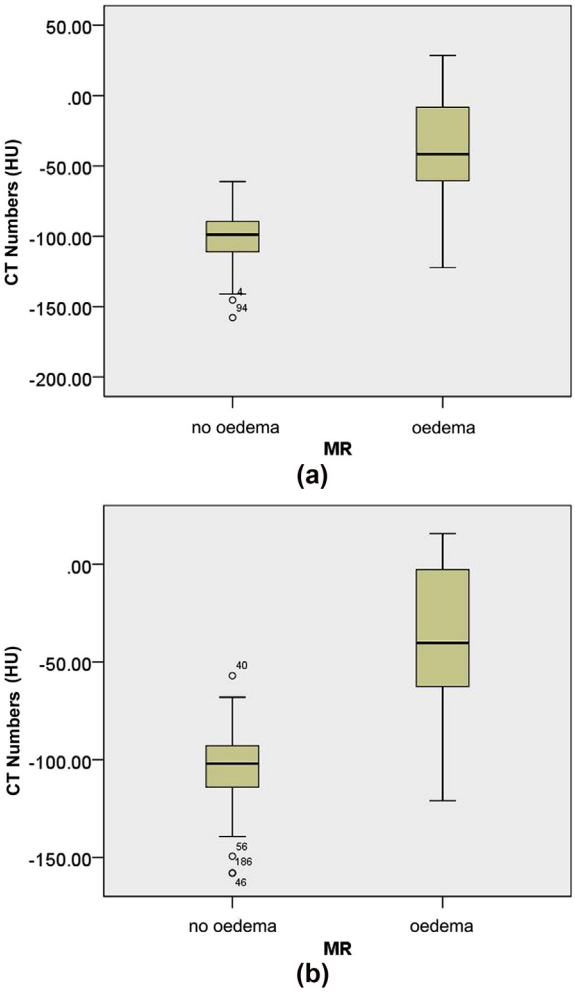

Figure 3 Box and whisker plots show mean dual-energy attenuation measured on VNCa images for all knee joint regions from reader 1 (a) and reader2 (b), taking MRI images as the reference standard.

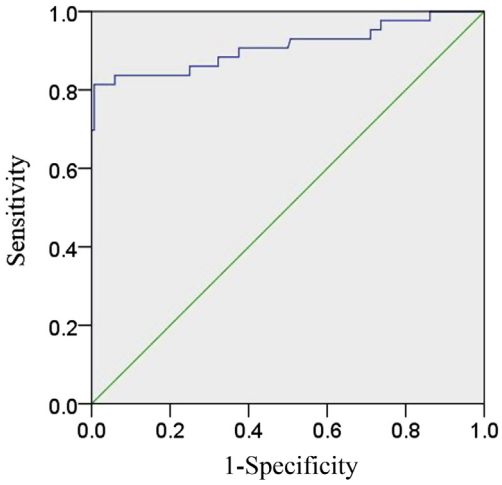

Figure 4 Graph shows the ROC curves calculated from the average attenuation derived from dual-energy colour-coded images of both readers with and without bone marrow oedema on MRI images. The area under the curve was 0.910.

Detection of post-traumatic bone marrow lesions in the knee joints with dual-energy CT was first reported by Pache *et al.*[11] Their study was conducted by using the first-generation dual-energy CT. Compared with results of their study, the present investigation did not evaluate the femur and tibia separately. A total specificity of 99.3% was obtained in the quantitative dual-energy CT analysis, which is more promising than the specificities of 97.9% and 91.5% reported in femur and tibia, respectively, by Pache *et al.* A sensitivity of 81.4% is higher than sensitivity of 78.9% in the femur, but lower than 95% in the tibia from their study. This may have resulted from a much younger mean age in the present than in their study population, and different amounts of red and yellow marrow in the femur and tibia; however, it may possibly strengthen the clinical effect of the present study results. Instead of assessing bone marrow oedema with grey-scale VNCa images like Pache *et al.*, the present study used colour-coded images for statistical analysis more intuitive. The area of bone marrow oedema was measured on dual-energy CT colour-coded images and MRI images to quantitatively analyse the accuracy of the range. MRI is the most sensitive technique to show bone marrow oedema. Consequently, the area of bone marrow oedema on the MRI images may be bigger than on dual-energy CT colour-coded images; however, statistical results showed that there was no significant difference

Table 3
Areas of oedematous regions on the magnetic resonance imaging (MRI) and dual-energy computed tomography (CT) images

	Area (mm^2)
MRI images (n=38)	6.75±4.79
Dual-energy CT images (n=38)	6.01±3.64
p-Value[a]	0.061

[a]p-Values were calculated with the pair t-test; $p<0.05$ indicates a significant difference.

between them, which indicates good diagnostic value of dual-energy CT. Although the *p*-value is not very high, it also indicated that there is a tendency to show consistency between the two methods to detect bone marrow. Further studies with a larger sample size could provide a more significant result.

For visual image evaluation, qualitative dual-energy CT analysis yielded a sensitivity of 88.4% and specificity of 98%, which are higher than the previous study results from different readers in Pache's study with sensitivities of 86.4% and 86.4% and specificities of 94.4% and 95.5%, respectively.[11] The optimal cut-off value of −67 HU was found in the present study. Pache *et al.* did not find a cut-off value for knee joints, but the value found in the present study was higher than the findings of Wang *et al.* (−80 HU) and lower than the findings of Petritsch *et al.* (−47 HU). The differences may result from the different parts of body, different scanners, different protocols, or different post-processing methods.

Five false-negative findings and three false-positive findings were observed during visual image assessment. The false-negative regions were those with slight bone marrow oedema or a small area of oedema making the changes in attenuation less pronounced. The smaller range of bone marrow oedema was easily concealed by artefacts, which makes it difficult to distinguish on colour-coded dual-energy images. The false-positive regions were mostly located near the articular surface, which were mistaken for bone marrow oedema on colour-coded images because of the influence of joint effusion or the incomplete removal of calcium due to the thicker cortex.

The present study had several limitations. Firstly, only a small number of patients was included in the present study, and so the statistical analysis could be underpowered; a large sample size is required for further evaluation. Secondly, the range of interval periods between the dual-energy CT and MRI examinations was large (mean interval, 2.1 days; range, 0–5 days). Although such thresholds are standard in clinical practice, this may have led to difference in findings as a result of alterations in the presence of bone oedema. Thirdly, age-related factors were not considered in the present study. Bone marrow composition is different due to the conversion of red to yellow marrow during growth and development,[2,22,23] which may affect the study results. A further study grouped according to age should be implemented in the future. Fourthly, the sections selected for area measurement of bone oedema may be not the same regions on both dual-energy CT colour-coded images and T2-weighted MRI images; however, axial dual-energy CT colour-coded images were reformatted by referring to the MRI parameters to reduce the influence of section selection.

In conclusion, the findings of the present study showed that bone marrow oedema could be diagnosed on dual-energy CT colour-coded images with a high sensitivity, specificity, and accuracy when compared with MRI. Dual-energy CT can serve as an alternative option for patients with contraindications to MRI.

Conflict of interest

The authors declare no conflict of interest.

Acknowledgement

The authors thank Ying-Qian Ge (Siemens Healthineers, Erlangen, Germany) for providing valuable technical assistance.

References

1. Thiryayi WA, Thiryayi SA, Freemont AJ. Histopathological perspective on bone marrow oedema, reactive bone change and haemorrhage. *Eur J Radiol* 2008;**67**(1):62–7 https://doi.org/10.1016/j.ejrad.2008.01.056.
2. Barr MS, Anderson MW. The knee: bone marrow abnormalities. *Radiol Clin North Am* 2002;**40**(5):1109–20 https://doi.org/10.1016/s0033-8389(02)00051-9.
3. Sanders TG, Medynski MA, Feller JF, *et al*. Bone contusion patterns of the knee at MRI: footprint of the mechanism of injury. *RadioGraphics* 2000;**20**:S135–51 https://doi.org/10.1148/radiographics.20.suppl_1.g00oc19s135.
4. Vincken PW, Ter Braak BP, van Erkel AR, *et al*. Clinical consequences of bone bruise around the knee. *Eur Radiol* 2006;**16**(1):97–107 https://doi.org/10.1007/s00330-005-2735-8.
5. Yao L, Lee JK. Occult intraosseous fracture: detection with MRI. *Radiology* 1988;**167**(3):749–51 https://doi.org/10.1148/radiology.167.3.3363134.
6. Thomas C, Schabel C, Krauss B, *et al*. Dual-energy CT: virtual calcium subtraction for assessment of bone marrow involvement of the spine in multiple myeloma. *AJR Am J Roentgenol* 2015;**204**(3):W324–31 https://doi.org/10.2214/ajr.14.12613.
7. Boks SS, Vroegindeweij D, Koes BW, *et al*. Follow-up of occult bone lesions detected at MRI: systematic review. *Radiology* 2006;**238**(3):853–62 https://doi.org/10.1148/radiol.2382050062.
8. Johnson TR, Krauss B, Sedlmair M, *et al*. Material differentiation by dual energy CT: initial experience. *Eur Radiol* 2007;**17**(6):1510–7 https://doi.org/10.1007/s00330-006-0517-6.
9. McCollough CH, Leng S, Yu L, *et al*. Dual- and multi-energy CT: principles, technical approaches, and clinical applications. *Radiology* 2015;**276**(3):637–53 https://doi.org/10.1148/radiol.2015142631.
10. Omoumi P, Verdun FR, Guggenberger R, *et al*. Dual-energy CT: basic principles, technical approaches, and applications in musculoskeletal imaging (part 2). *Semin Musculoskel Radiol* 2015;**19**(5):438–45 https://doi.org/10.1055/s-0035-1569252.
11. Pache G, Krauss B, Strohm P, *et al*. Dual-energy CT virtual non-calcium technique: detecting posttraumatic bone marrow lesions—feasibility study. *Radiology* 2010;**256**(2):617–24 https://doi.org/10.1148/radiol.10091230.
12. Guggenberger R, Gnannt R, Hodler J, *et al*. Diagnostic performance of dual-energy CT for the detection of traumatic bone marrow lesions in the ankle: comparison with MRI. *Radiology* 2012;**264**(1):164–73 https://doi.org/10.1148/radiol.12112217.
13. Wang CK, Tsai JM, Chuang MT, *et al*. Bone marrow edema in vertebral compression fractures: detection with dual-energy CT. *Radiology* 2013;**269**(2):525–33 https://doi.org/10.1148/radiol.13122577.
14. Petritsch B, Kosmala A, Weng AM, *et al*. Vertebral compression fractures: third-generation dual-energy CT for detection of bone marrow edema at visual and quantitative analyses. *Radiology* 2017;**284**(1):161–8 https://doi.org/10.1148/radiol.2017162165.
15. Suh CH, Yun SJ, Jin W, *et al*. Diagnostic performance of dual-energy CT for the detection of bone marrow oedema: a systematic review and meta-analysis. *Eur Radiol* 2018;**28**(10):4182–94 https://doi.org/10.1007/s00330-018-5411-5.
16. Kellock TT, Nicolaou S, Kim SSY, *et al*. Detection of bone marrow edema in nondisplaced hip fractures: utility of a virtual non-calcium dual-energy CT application. *Radiology* 2017;**284**(3):922 https://doi.org/10.1148/radiol.2017161063.

17. Liu X, Yu L, Primak AN, *et al*. Quantitative imaging of element composition and mass fraction using dual-energy CT: three-material decomposition. *Med Phys* 2009;**36**(5):1602–9 https://doi.org/10.1118/1.3097632.
18. Coursey CA, Nelson RC, Boll DT, *et al*. Dual-energy multidetector CT: how does it work, what can it tell us, and when can we use it in abdominopelvic imaging? *RadioGraphics* 2010;**30**(4):1037–55 https://doi.org/10.1148/rg.304095175.
19. Landis JR, Koch GG. The measurement of observer agreement for categorical data. *Biometrics* 1977;**33**(1):159–74 https://doi.org/10.2307/2529310.
20. Cyr L, Francis K. Measures of clinical agreement for nominal and categorical data: the kappa coefficient. *Comput Biol Med* 1992;**22**(4):239–46 https://doi.org/10.1016/0010-4825(92)90063-s.
21. Johnson TR. Dual-energy CT: general principles. *AJR Am J Roentgenol* 2012;**199**(Suppl. 5):S3–8 https://doi.org/10.2214/ajr.12.9116.
22. Vogler 3rd JB, Murphy WA. Bone marrow imaging. *Radiology* 1988;**168**(3):679–93 https://doi.org/10.1148/radiology.168.3.3043546.
23. Laor T, Jaramillo D. MRI insights into skeletal maturation: what is normal? *Radiology* 2009;**250**(1):28–38 https://doi.org/10.1148/radiol.2501071322.